

Volume Computation of 3D Reconstructed Models from Volumetric Data using Binary Indexed Tree

Nguyen Le Quoc Bao & Le Tuan Hy

8 March 2024

Abstract

In the burgeoning field of medical imaging, precise computation of 3D volume holds a significant importance for subsequent qualitative analysis of 3D reconstructed objects. Combining multivariable calculus, marching cubes algorithm, and binary indexed tree data structure, we develop an algorithm for efficient computation of intrinsic volume of any volumetric data retrieved from computed tomography (CT) or magnetic resonance (MR). We proposed the 30 configurations of volume values based on polygonal mesh generation method. Our algorithm processes the data in scan-line order simultaneously with reconstruction algorithm to create a Fenwick tree, ensuring query time much faster and assisting users' edition of slicing or transforming model. We tested the algorithm's accuracy on simple 3D objects (e.g. sphere, cylinder) to complicated structures (e.g. lungs, cardiac chambers). The result deviated within $\pm 0.004\text{cm}^3$ and there is still space for further improvement.

1 Introduction

In the contemporary landscape of medical imaging, the conversion of tomographic data into precise three-dimensional (3D) models stands as a burgeoning trend of paramount importance. This evolution necessitates robust post-processing methodologies to ensure the meticulous measurement and analysis of these intricate 3D structures with utmost accuracy and efficiency [1]. Of particular significance is the quantification of various parameters within the cardiovascular system, including but not limited to the diameter, area, and volume of critical structures such as the aortic duct. These metrics serve as pivotal indicators for pathologies such as hypertrophy or stenosis, which pose significant risks to patient well-being. Consequently, the accurate assessment and preoperative planning facilitated by such analyses substantially enhance the clinical efficacy and safety of surgical interventions. Notwithstanding the strides made in tomographic reconstruction software, the precise volumetric measurement of 3D cardiac models remains an enduring challenge, underscoring the persistent absence of a definitive solution within the current

landscape of medical imaging technologies. While existing software proficiently translates medical tomographic data into comprehensive 3D representations, the capability to perform volumetric analysis remains conspicuously absent, thereby warranting further advancements in this critical domain.

1.1 Data flow in algorithms

3D medical image reconstruction consists of 6 steps. The last feature is optional since it depends on the software application offering user advanced operations.

- Data Acquisition

- Image Processing

- Segmentation

- 3D Reconstruction

- Rendering & display

- Post processing

2 Literary review

Researchers have reported the application of 3D medical images in a variety of areas. The visualization of complex acetabular fractures, craniofacial

abnormalities, and intracranial structure illustrate 3D's potential for the study of complex bone structures. Applications in radiation therapy and surgical planning interactive 3D techniques combined with 3D surface images. Cardiac applications include artery visualization and non-graphic modeling applications to calculate surface area and volume. There is non-graphic modeling applications to calculate the surface area and volume of cardiac models in 1985 [2].

3 Methodology

Since our main application is in medical imaging, we only focus practical experiment and analysis in medical field. Since medical models are more complicated in structures than any other 3D models, our method proves superior performance in many kinds of volumetric data in the experiment section.

3.1 Integral of surface functions

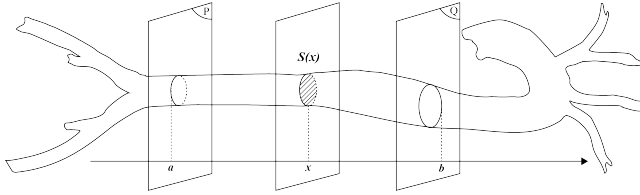


Figure 1: Calculating the volume of the aortic duct by integrating the surface function

We can determine whether the arterial duct is hypertrophied by comparing its volume to standard parameters. We intersect the aorta with two planes $(P), (Q)$ using a symmetric ray Casting method [3]. The limits a, b on the Ox axis of an object are $(x = a, x = b, a \leq b)$. A plane perpendicular to the Ox axis at point x and $a \leq x \leq b$ intersects the object with a cross-sectional area of $S(x)$ and the equation $S(x)$ is continuous on the interval $[a; b]$. Thus, the volume of the upper heart chamber is calculated by the following integral formula:

$$V = \int_a^b S(x)dx$$

For a set of n slice images, we have S_i as the area of the i_{th} slice ($1 \leq i \leq n$). Approximating a function $S(x)$ is not straightforward. We can use the Lagrange interpolation method. However, this approach has many limitations. Firstly, the

approximation is only accurate if $n \rightarrow \infty$ to ensure accuracy. This is practically infeasible because the number of slices n is usually not large enough ($300 \rightarrow 512$) and is limited. Secondly, approximating a function is also a complex task, increasing algorithm's processing time.

3.2 Inclusion and exclusion principle

Double integral problem is a combination of multiple single integral problems. Initially, we divide the curved surface $z = f(x, y)$ into surfaces S_j, S_{j+1}, \dots, S_m corresponding to each y_j, y_{j+1}, \dots, y_m where each surface S_j with fixed y_j represents a single integral problem. Finally, we sum up these surfaces S_j to calculate the volume V :

$$D = \begin{cases} a \leq x \leq b \\ c \leq y \leq d \end{cases}$$

$$V = \int_c^d \left(\int_a^b f(x, y) dx \right) dy = \int_c^d dy \int_a^b f(x, y) dx$$

With inclusion and exclusion principal, we can measure the volume of predetermined structure. For example, When calculating the volume of the aortic arch, we divide this vessel into two parts: the upper half o_1 and the lower half o_2 so the domain D remains the same. The volume of the inner part will be $V_o = V_{o_1} - V_{o_2}$:

$$V_o = V_{o_1} - V_{o_2}$$

$$V_o = \lim_{\Delta x_i, \Delta y_j \rightarrow 0} \sum_{j=c}^{j=d} \left(\sum_{i=a}^{i=b} (z_{ij}^{o_1} - z_{ij}^{o_2}) \Delta x_i \right) \Delta y_j$$

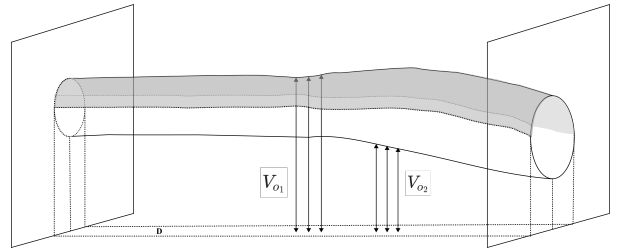


Figure 2: Calculating partial aortic arch volume with double integral

The implementation of this approach computed the volume of tube structures accurately (given the (x, y, z) point set). However, we have to find a mid-section to divide the object into two parts. Additionally, current software systems [3] allows radiologists to perform surgical operations (e.g. slicing) or

modifies the segmentation result leading to changes in the 3D reconstructed polygonal mesh, so algorithm must reprocess again. If denoting Q as the times of slicing or updating operation is performed, the time complexity will be $O(Q \times (M \times N + S))$, where S represents the complexity of finding midsection path. This issue can be optimized with triple integral combined with binary indexed tree.

3.3 Triple integral

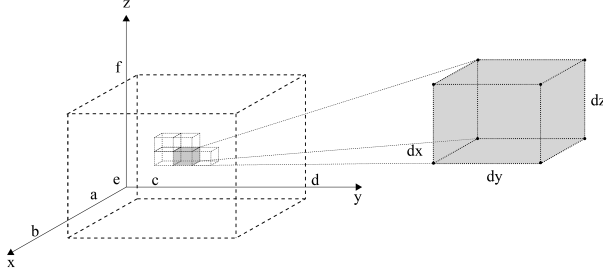


Figure 3: Calculating the volume of an object with triple integration

The concept of triple integration originates from dividing the object volume O into n very small rectangular prisms or cubes O_i with lengths, widths, and heights denoted as dx, dy, dz respectively. Approximating the volume of the original object is straightforward by summing the volumes of all O_i with $1 \leq i \leq n$ and as $n \rightarrow +\infty$:

$$V = \lim_{n \rightarrow +\infty} \sum_{i=1}^n \Delta z_i \Delta y_i \Delta x_i$$

The above formula shows that each cube is processed in three loops of three dimension x, y, z , which is comprehensively compatible with the marching algorithm. Therefore we integrate the approximation idea of triple integral into marching cubes algorithm and store the calculated data into 3D binary indexed tree.

3.4 Volume configurations in Marching Cubes

Marching cubes uses a divide-and-conquer approach to locate the surface in a logical cube created from eight pixels; four each from two adjacent slices [4]. In three dimensional space, the relationship between

a cube and the 3D model falls into three cases: the cube is totally inside the model, partly intersected by the surface model, or totally located outside the model. The surface can intersect the cube in $2^8 = 256$ cases since a cubes has 8 vertices in total (this can be proved by generation method).

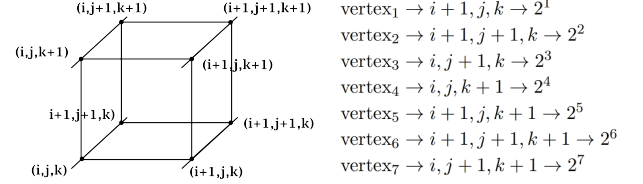


Figure 4: Vertex indexing and binary representation

However, [4] reduced the problem from 256 cases to 14 patterns by utilizing symmetrical property, rotational symmetry. From original 3D array, the algorithm create the boolean 3D array with the same size speculating that a vertex is false if locates inside the model and vice versa. Therefore, the volume of the model within a cube is limited from the mesh generated to all False vertices. Although the topology triangulated mesh is unchanged when performing rotation or symmetrical operations [4], the volume is changed. Specifically, the volume of case j is equal to $1 - V_i$ with j is the reversed case of i . Finally, we have up to 28 cases of volume plus 2 cases (all vertices are either False or True), which totally is 30 cases. The specified volume of each 30 cases is presented in figure 4.

The volume is each case easily calculated by dividing the 3D shape into simple shapes such as tetrahedron, prism,... The formulas are:

$$V_{\text{tetrahedron}} = \frac{1}{3} h S_{\text{base}}$$

$$V_{\text{prism}} = h S_{\text{base}}$$

With more complicated reconstructed mesh, we assigned coordinates to the cubes and use vectors operations (e.g. dot-product, cross-product). For example, given 4 points $A(x_A, y_A, z_A)$, $B(x_B, y_B, z_B)$, $C(x_C, y_C, z_C)$, $D(x_D, y_D, z_D)$, we have:

$$V_{ABCD} = \frac{1}{6} |\vec{AB} \times \vec{AC}| \cdot \vec{AD}$$

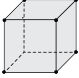
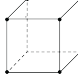
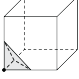
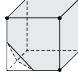
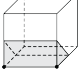
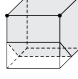
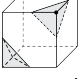
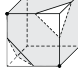
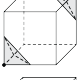
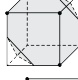
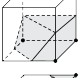
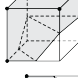
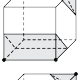
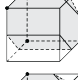
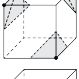
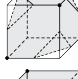
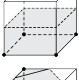
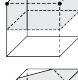
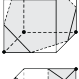
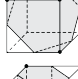
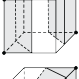
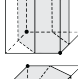
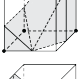
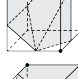
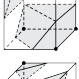
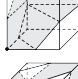
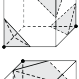
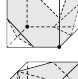
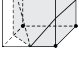
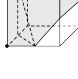
Cases	Calculation	Explanation	Volume	Reversed case	Reversed Volume
	$1 \times 1 \times 1$	1 cube	1		0
	$\frac{1}{3} \times 0.5 \times \frac{1}{2} \times 0.5^2$	1 tetrahedron	$\frac{1}{48}$		$\frac{47}{48}$
	$1 \times \frac{1}{2} \times 0.5^2$	prism	$\frac{1}{8}$		$\frac{1}{8}$
	$2 \times \frac{1}{48}$	2 tetrahedrons	$\frac{1}{24}$		$\frac{23}{24}$
	$2 \times \frac{1}{48}$	2 tetrahedrons	$\frac{1}{24}$		$\frac{23}{24}$
	$\frac{1}{4} + \frac{1}{12} + \frac{1}{48}$	1 prism, 2 tetrahedrons	$\frac{17}{48}$		$\frac{31}{48}$
	$\frac{1}{8} + \frac{1}{48}$	1 prism, 1 tetrahedron	$\frac{7}{48}$		$\frac{41}{48}$
	$3 \times \frac{1}{48}$	3 tetrahedrons	$\frac{1}{16}$		$\frac{15}{16}$
	$\frac{1}{2}$	half of 1 cube	$\frac{1}{2}$		$\frac{1}{2}$
	$\frac{1}{2}$	half of 1 cube	$\frac{1}{2}$		$\frac{1}{2}$
	$2 \times \frac{1}{8}$	2 prisms	$\frac{1}{4}$		$\frac{3}{4}$
	$\frac{1}{8} + \frac{1}{12} + \frac{1}{6} + \frac{1}{8}$	1 prism, 3 tetrahedrons	$\frac{1}{2}$		$\frac{1}{2}$
	$\frac{1}{48} + \frac{17}{48}$	1 prism, 3 tetrahedrons	$\frac{139}{144}$		$\frac{5}{144}$
	$4 \times \frac{1}{48}$	4 tetrahedrons	$\frac{1}{12}$		$\frac{11}{12}$
	$\frac{1}{8} \times 3 + \frac{1}{24}$	2 prisms, 2 tetrahedrons	$\frac{5}{12}$		$\frac{7}{12}$

Table 1: Volume of 3D model within a cube specification for 30 cases (15 configurations)

However the Marching Cube method proposed by [4] has limitations. The algorithm can lead to cracks because the same configuration can be tiled in different ways [5]. Lewiner optimized the algorithm by considering more cases (32 base cases instead of 15). However, in our research scope, we only speculate the volume based on Lorensen’s lookup table to estimate the practicability of our assumption before further improvement with Lewiner’s extended one.

The vertex with bold black dot is the false one, which means this vertex possesses value below the threshold level and is totally inside the 3D reconstructed polygonal mesh. The volume of the model within each cube need considering is highlighted from the initial 15 base cases to next 15 reversed cases with calculation formulas, explanation, and results provided simultaneously. Specially, in the last 5 cases (four False vertices and four True vertices), although not only the topological mesh configuration but also the vertices relative position remain unchanged while being reversed, the intrinsic volume essentially changes. Therefore when speculating volume configurations for 256 cases (for fast query), we use the vertex₀(x, y, z) as pivot to classify case 26, 27, 28, 29, 30 from case 11, 12, 13, 14, 15.

Considering implementation, supposing the volumetric data named is specified in size (N, M, P), we initialize a 3D array named Cube of size ($N - 1, M - 1, P - 1$). We take the vertex₀(x, y, z) as pivot to manage the whole cube or 7 last other vertices ($x + 1, y, z$), ..., ($x + 1, y + 1, z + 1$). Therefore, Cube[i, j, k] = VolumeLookup(i, j, k) with $i \leq N - 1, j \leq M - 1, k \leq P - 1$ and VolumeLookup returns the volume based on above 30 cases.

Finally, we can sum up all the value in this 3D array to get the total volume of our 3D object. However, this way of storing calculation results is not suitable when updates (e.g slicing, mesh edition) occur. The time complexity is $O(Q \times N \times M \times P)$ with Q is the number of update events.

3.5 Binary indexed tree

The Binary indexed tree (BIT), also Fenwick Tree, is a widely used data structure in competitive programming, introduced in the research paper "A new data structure for cumulative frequency tables" by Peter M. Fenwick [6]. The BIT exhibits the following characteristics: querying the result of a subprob-

lem in $O(\log N)$, updating the value for one element in $O(\log N)$, or a segment in $O(N \log N)$, low memory usage $O(N)$, and fast processing speed (due to bitwise operations). In detail, with each update operation, the last bit is always shifted up at least 1 time, leading to the maximum of $\log N$ times of bit shifts.

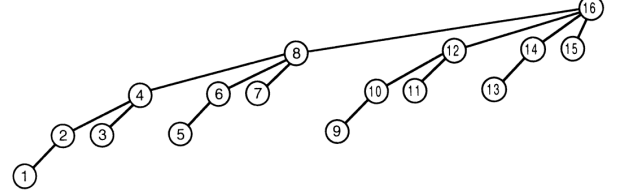


Figure 4: The updating binary indexed tree [6]

In BIT, the element i_{th} stores the result $F[i]$ of the subproblem containing 2^k elements starting/ending at position i , where k is the lowest set bit in the binary representation of i . Observing the representation of the tree above, we can easily see that nodes with odd indices manage only themselves, while nodes with index id will have a parent with index $id + 2^k$. Finding the value of 2^k is simply done by performing the bitwise operation: $2^k = -id \& id$.

3.5.1 3D Binary indexed tree

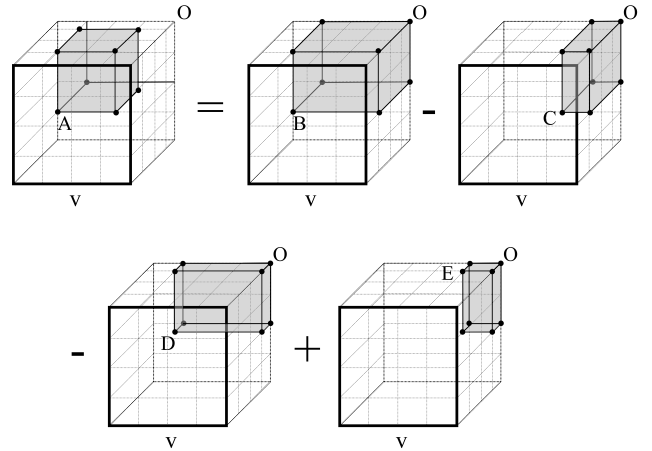


Figure 5: Query a region in 3D BIT

This is a novel application of binary indexed trees into three-dimensional arrays. We employ the principle of inclusion and exclusion to query the sum of elements over a 3D space by excluding surrounding parts, similar to slicing but without data loss). We can perform updates on a 3D space (altering the mesh reconstruction) with minimal complexity of $O(\log N \times \log M \times \log P)$, where (N, M, P) repre-

sent the dimensions of volumetric data. The formula of 3D query is:

$$\begin{aligned}
Q(x1, y1, z1, x2, y2, z2) = & S(x2, y2, z2) \\
& -S(x2, y2, z1 - 1) - S(x2, y1 - 1, z2) \\
& +S(x2, y1 - 1, z1 - 1) - S(x1 - 1, y2, z2) \\
& +S(x1 - 1, y2, z1 - 1) + S(x1 - 1, y1 - 1, z2) \\
& -S(x1 - 1, y1 - 1, z1 - 1)
\end{aligned}$$

Q , S represent the QueryByRegion and getSum function respectively in the implementation code. In the marching cubes three loop, instead of storing data into 3D array Cube, we build cumulatively the BIT by calling update function as $BIT[i, j, k] = update(i, j, k, value)$ with $value$ is the VolumeLookup(i, j, k).

You can find the open-source code published online on Github in the Open Source section.

4 Experiments

4.1 Setup experiments

We experimented our algorithm both on simple shape (sphere) with predetermined radius and complex 3D structure (cardiac model) with predetermined volume. The computed volume and labelled volume is represented in table 2. Also, we compare the time processing of BIT query with brute force method. Each case is computed 5 times to ensure consistency. In medical imaging, especially dealing with volumetric data acquired from CT, MR. We have to consider the pixel spacing value, slice thickness for accurate unit conversion from pixel/voxel world into real world unit (mm^3 or ml). We run the algorithm only with CPU.

4.2 Results and evaluation

Observing the table 2, the Brute Force (BF) time increases correspondingly with the size of volumetric data. However, by query the BIT tree with Cython implementation, the time of query of any part is only 0.0. You can find the open-source code and run yourself to reconfirm. The more high-resolution the volumetric data is, the more accurate of calculated volume we can approximate. Meanwhile, with medical volumetric data (cardiac structures), the

Processing time represents both time dedicated to Marching Cubes and BIT initialization. Our Marching cubes implementation is basic, prolonging the processing time.

4.3 Results and evaluation

5 Open Source

We implemented the Marching Cubes algorithm based on Lorensen’s lookup table instead of Lewiner’s. We initialized two lookup table volume configurations named VOLUME_CASE_LOOKUP of size 30 and VOLUME_LOOKUP of size 256. We implemented the code with Cython, an efficient Python to C compiler, to optimize performance. This approach allowed us to efficiently handle the volume rendering process, ensuring accurate results while maintaining computational efficiency. We also published the pure Python code of the algorithm. However, the pure Python code should only be used for small-sized 3D arrays. For medical volumetric data, especially high-resolution ones, it’s recommended to utilize the C/C++ implementation or use Cython.

Code link: <https://github.com/WISEF-ISEF-team/Volume-Computation-of-3D-Reconstructed-Models-from-Volumetric-Data-using-Binary-Indexed-Tree.git>

Shape	Radius	BIT time (s)	BF time (s)	Cal V (cm ³)	La V (cm ³)
$50 \times 50 \times 50$	10	0.0	0.026	2.573	2.645
	15	0.0	0.016	8.546	8.929
	20	0.0	0.015	20.079	21.166
	25	0.0	0.020	39.120	41.340
$100 \times 100 \times 100$	20	0.0	0.151	20.668	21.166
	25	0.0	0.154	8.546	41.340
	30	0.0	0.168	69.535	71.435
	35	0.0	0.155	110.428	113.436
$250 \times 250 \times 250$	20	0.0	2.284	71.195	71.435
	25	0.0	2.174	112.879	113.436
	30	0.0	2.295	168.133	169.328
	35	0.0	2.224	239.140	241.094
$500 \times 500 \times 500$	20	0.0	19.962	21.197	21.166
	25	0.0	19.193	71.408	71.435
	30	0.0	18.946	169.2042	169.328
	35	0.0	19.714	240.021	241.094

Table 2: Experiment on sphere

Structure	Shape	Processing time (s)	Cal V (ml)	La V (ml)
Left ventricle	$512 \times 600 \times 600$	127.960	120.06618	100-140
Right ventricle	$512 \times 600 \times 600$	126.965	75.08047	50-100
Left atrium	$512 \times 600 \times 600$	103.747	30.93378	25-35
Right atrium	$512 \times 600 \times 600$	102.356	100.00465	80-110
Myocardium	$512 \times 600 \times 600$	108.042	183.84389	
Ascending aorta	$512 \times 600 \times 600$	204.393	25.047446	20-30
Descending aorta	$512 \times 600 \times 600$	275.57	125.333	100-150
Pulmonary trunk	$512 \times 600 \times 600$	244.903	26.249936	20-30
Vena cava	$512 \times 600 \times 600$	169.776	107.07984	
Auricle	$512 \times 600 \times 600$	175.576	12.508784	10-15
Coronary Artery	$512 \times 600 \times 600$	114.604	13.09273	

Table 3: Experiment on cardiac volumetric data

References

- [1] K. Schladitz, J. Ohser, and W. Nagel, “Measuring intrinsic volumes in digital 3d images,” in *Discrete Geometry for Computer Imagery: 13th International Conference, DGCI 2006, Szeged, Hungary, October 25-27, 2006. Proceedings 13*. Springer, 2006, pp. 247–258.
- [2] E. A. Hoffman and E. L. Ritman, “Shape and dimensions of cardiac chambers: importance of ct section thickness and orientation.” *Radiology*, vol. 155, no. 3, pp. 739–744, 1985.
- [3] N. Bao and L. Hy, “Integration of deep learning into automatic cardiovascular volumetric dissection and reconstruction in 3d simulated space for medical practice,” 2024.
- [4] W. E. Lorensen and H. E. Cline, “Marching cubes: A high resolution 3d surface construction algorithm,” in *Seminal graphics: pioneering efforts that shaped the field*, 1998, pp. 347–353.
- [5] T. Lewiner, H. Lopes, A. W. Vieira, and G. Tavares, “Efficient implementation of marching cubes’ cases with topological guarantees,” *Journal of graphics tools*, vol. 8, no. 2, pp. 1–15, 2003.
- [6] P. M. Fenwick, “A new data structure for cumulative frequency tables,” *Software: Practice and experience*, vol. 24, no. 3, pp. 327–336, 1994.